ATOMIZATION OF GEL PROPELLANTS THROUGH AN AIR-BLAST TRIPLET ATOMIZER

Shai Rahimi

RAFAEL/MANOR Propulsion and Explosive Systems Division, Haifa, Israel

Benveniste Natan*

Faculty of Aerospace Engineering, Technion - Israel Institute of Technology, Haifa, Israel

ABSTRACT

An effort was made to relate the rheological properties of gel propellant simulants with their atomization behavior. The gels were atomized using a triplet impinging air-blast atomizer. The experimental investigation demonstrates that pseudoplastic water gels exhibit spray patterns that resemble those of Newtonian liquids, but they are more difficult to atomize. The Sauter mean diameter decreases along the injector axis and increases with increasing radial coordinate and the angle between the gas jets plane and the horizontal plane. Wide-angle convergent injectors require lower upstream pressure to achieve the same atomization performance with straight injectors. Sauter mean diameter decreases down to a minimum constant value with the increase of the air-to-liquid mass flow rate ratio. Sauter mean diameter increases with increasing gellant content due to the respective increase of the shear viscosity. An expression relating the Sauter mean diameter to the injection conditions and the mean apparent viscosity at the injector exit is presented.

* Corresponding author. Faculty of Aerospace Engineering, Technion - Israel Institute of Technology, Haifa 32000, Israel. e-mail: aerbeny@aerodyne.technion.ac.il

INTRODUCTION

Gel propellants are liquid fuels and oxidizers whose rheological properties have been altered by the addition of gelling agents and frequently, energetic solid additives, such that they behave as non-Newtonian time dependent fluids. In addition to the viscous branch, which is dominant in pure liquid propellants, elastic and plastic branches are supplemented to the propellant, as well as time dependent properties such as thixotropy. These propellants are advantageous over conventional liquids and solid propellants because of their capability of providing full energy management and because of their safety benefits. Their performance characteristics and operational capabilities, which are similar to liquid propellants, as well as their high density, increased combustion energy and long term storage capability, make them attractive for many applications, especially for volume-limited propulsion system applications.

During the past decades, many studies and patents covering different aspects of gel propulsion have been conducted. These studies focused mainly on gel propellants preparation processes, basic rheology and flow, atomization, combustion and energetic performance, applications and technological demonstrations, material compatibility and impulse intensification by metal content for space applications. A detailed survey of the work done on gel propellants is presented in the review paper of Natan and Rahimi [1].

The addition of gelling agents can prevent agglomeration, aggregation and separation of the metal-solid phase from the fuel during storage by constructing a new microstructure. However, this also causes the gel viscosity to increase, which makes the fuel more difficult to atomize and reach high combustion efficiency in rocket engines.

As regards gel propellant atomization, only a few, mainly qualitative works have been conducted. The atomization and the combustion of metallized gel slurry fuels for ramjet

applications have been studied by Netzer's group [2-3] at the Naval Postgraduate School, using commercial atomizers. Guglielmi [2] measured the Sauter mean diameter (SMD) of non-reactive spray and very coarse atomization was obtained in comparison to water under the same flow conditions (SMD was eight times larger). Guglielmi concluded that the air to liquid mass ratio (ALR) and pressure drop required for adequate atomization, are not feasible in a ramjet engine. Urbon [3] used an air-blast and an ultrasonic atomizer in both reactive and non-reactive flow conditions. Although the air-to-fuel ratio in the ultrasonic atomizer reached higher values than that required in the air-blast atomizer, the pressure drop needed was lower thus feasible for use in ramjet engines. Under regular ramjet combustor conditions, the ultrasonic atomizer provided sustained stable combustion, while the air-blast failed to sustain steady combustion. In NASA, Green et al. [4] provided a flow visualization of gel simulants using triplet and coaxial injectors. Photographic images of the spray patterns showed that the non-gelled liquid sprays produced finer and more uniform atomization than that of the gel and this was attributed to high apparent shear viscosity of the fluid, which was calculated for a constant strain rate at the exit of the injector. Chojnacki and Feikema [5-7] investigated the atomization of water gels using a like-on-like doublet injector and the fluid injection system was transformed to a capillary viscometer to measure the viscosity of the non-Newtonian gel. In a study on the non-Newtonian liquid sheets formed by impinging jets at several impingement angles, Chojnacki and Feikema [7], indicate that the breakup radius exhibits a general trend of increasing with increasing Weber number. An attempt was made to predict the wavelength of ligaments shed from a liquid sheet using linear stability analysis, which considers the non-Newtonian effect. However the analysis over-predicted the wavelength.

One of the most important characteristics of gel propellants is the fact that their viscosity tensor depends on both the strain-rate tensor and time. This dependency dictates coupling

between the flow field and the material properties, both affecting the spray characteristics. Very few works refer to the influence of *non-Newtonian* rheological properties on the atomization characteristics. Mansour and Chigier [8] investigated the air-blast atomization characteristics of non-Newtonian materials using a co-axial twin fluid atomizer. They provided a rheological characterization of the fluids that included shear and extensional viscosity measurements. Moreover, they connected the rheological properties with atomization characteristics and concluded that for shear-thinning, pseudoplastic fluids with low yield stress, the SMD depends on the shear rate. They indicated that the mass averaged shear viscosity seems to be the most appropriate choice to correlate against the atomization characteristics of non-Newtonian fluids (SMD). As regards viscoelastic materials, they were more difficult to atomize than the viscoinelastic ones, and they indicate that the extensional viscosity rather than the apparent (shear) viscosity "is the most significant rheological mechanism that inhibits breakup." Apparently, two scalar projections of the viscosity tensor can be taken into consideration as measurable parameters influencing the spray pattern, the shear viscosity and the extensional viscosity, indicating the viscous and the elastic branches respectively. The effect of the extensional viscosity on polymer solution sprays was investigated by Dexter [9]. He indicates that shear viscosities are significantly lower than the extensional viscosities. Therefore, the influence of the shear viscosity on the spray pattern is of minor importance. Taske and Bilanin [10] suggested that the Deborah number (De) should be considered for characterization of the spray properties. The flow characteristic time was defined by the injector diameter divided by the relative gas-liquid velocity. However, the fluid characteristic time was not defined for a non-Newtonian liquid spray. Yarin et al. [11] studied the rheological behavior of gelled propellant simulants similar to those used in the present research, in uniaxial, elongational flow. They demonstrated that the three-dimensional power-law model permits description of uniaxial elongation and that the values

of the rheological parameters in simple shear and in uniaxial elongation agree fairly closely. Some other examples of power-law model validation in both elongation and shear were reported [12] for a number of suspensions.

Injection of the gel propellant through a converging injector causes the shear rate to increase due to fluid acceleration, consequently resulting in a decrease of the shear viscosity along the injector axis. Rahimi and Natan developed a simplified theoretical model [13] and a numerical model [14] for the flow field of a non-Newtonian fluid in a tapered tube injector. Their results show that increasing the convergence angle may reduce significantly the exit cross-section mean apparent viscosity of the flow. The thixotropic effect was investigated by Rahimi and Natan [15] for inorganic gel fuels. The results indicated that the thixotropic effect is insignificant for these kinds of fluids in typical propulsion feed system time constants.

In the present work, basic experimental data on the atomization of gel propellants using a triplet impinging air-blast injector with a central converging gel orifice are presented. An effort was made to include the effects of measured rheological parameters, the injector geometry and the control parameters of the injection system on spray characteristics.

EXPERIMENTAL SETUP

The experimental system (Fig. 1) consists of three major parts: the propellant (gel fuel and gaseous oxidizer simulant) feeding system, the injection system, and the droplet size measurement and data acquisition system.

The gel feeding system is designed to bring a planned continuous flow of gel fuel to the injector entrance with insignificant alteration to the rheological properties of the fluid. The gel fuel is stored in a 4.6 lt cylinder with a hydraulically operated, 100 mm diameter piston. The downstream end of the cylinder is connected by a flexible pipe to the injector housing.

The upstream part, behind the piston, contains hydraulic fluid, necessary for the gel fuel mass flow rate measurement. Since gels behave as non-Newtonian fluids with physical properties that depend on the flow conditions and may change with time, it is almost impossible to measure the gel mass flow rate by any direct interference in the gel flow. Two methods are used to establish the gel fuel mass flow rate: by measuring the piston movement by a linear potentiometer and by measuring the flow rate of the hydraulic fluid by a turbine flowmeter. The hydraulic fluid is stored in a 6 lt, nitrogen-pressurized tank. The gel feed system is designed to withstand pressures up to 180 atm.

The injection system is designed to produce a continuous gel spray for various atomizer types and allow temperature and atomizer pressure drop measurements. Gaseous nitrogen is used as an oxygen simulant. The nitrogen mass flow rate is measured by a standard sonic orifice. The injector housing is located on an X-Y-Z mounting unit that allows movement of a mass up to 30 kg by 40-50-15 cm respectively, as well as different axial head positioning. This enables control of the droplet size measurement location while the Malvern Mastersizer stays in place (Fig.2). The injector housing transfers the fuel gel and the nitrogen flow to the atomizer that produces the spray.

In the present investigation triplet air-blast atomizers with various geometries are used. The atomizer geometry is shown in Fig. 3. The nitrogen flow passes through two, 2 mm diameter, 15 mm length, cylindrical passages with impingement angles $\beta=50^{o}$-80^{o}. The distance between the impinging point and the injector face plate, L, has been held constant for each test set. The gel passes through an 8 mm length converging passage with various convergence angles, α. The exit diameter varied between 0.42-1.6 mm. The measurements were taken at the centerline at a distance of 2 or 6 cm downstream of the injector plane.

A Malvern Mastersizer X is used for the droplet size measurements. Mastersizer X is capable of measuring multi-modal droplet distributions of sizes between 1.2-600 μm. A 2 mW, He-

Ne laser produces a collimated, 18 mm diameter, 0.633 μm wavelength beam of light that illuminates the droplets. The incident light is diffracted by the droplets to give a stationary diffraction pattern independent of particle position and velocity. The scattered light is focused onto a 31-element, circular photo-diode array by a Fourier transform lens. A Malvern provided Windows software based on Mie laser diffraction theory is used for the data analysis.

Steady state flow conditions were employed during droplet size measurements. These were made during a period of 2 s with a sampling rate of 500 Hz. Pressures and mass flow rates were measured for 20 s with a sampling rate of 5 Hz. Experimental uncertainties were estimated by the small-sample method as less than 2% for the gel mass flow rate and less than 1% for the gas flow rate.

The rheological properties of the gel propellant simulants used in the present research were measured by a TA CSL^2_{100} Carri-Med Rheometer using cone and plate geometry. The existence of no-slip conditions during the measurements was verified. Special procedures were implemented to eliminate air-friction parasitic moments and inertia effects due to the rotating rheometer parts and also gap variations due to thermal changes.

RHEOLOGICAL CHARACTERIZATION OF GEL PROPELLANT SIMULANTS

The purpose of the rheological characterization was to typify the rheological nature of the atomized fluids and to quantify the influence of physical and kinematic parameters on their dominant properties where relevant to the injection processes.

The water gels were prepared using Carbopol-EDT^{TM} 2050 as the gelling agent.

The flow curves of water gel simulants with different gelling agent content are presented in Fig. 4. It can be concluded from these curves that the water gel simulant can be characterized as pseudoplastic, shear-thinning material. The power-law and the Herschel-Bulkley models,

described in one-dimensional form by Eqs. (1) and (2) respectively, were fitted to the shear viscosity versus shear rate curves shown in Fig. 4. The rheological parameters were obtained for a wide range ($8x10^{-4}$-$2x10^{3}$ s^{-1}) of shear rates and are summarized in Table 1.

$$\tau = K\dot{\gamma}^{n} \tag{1}$$

$$\tau = \tau_{HB} + K\dot{\gamma}^{n} \tag{2}$$

The shear viscosity for power-law fluids is given by:

$$\eta = K\dot{\gamma}^{n-1} \tag{3}$$

It is rather obvious that the power-law model cannot describe adequately the fluid behavior in the low shear rate range. Yield stress was estimated using indirect and direct techniques, based on the Herschel-Bulkley model and rheometer sensitivity. However, since the yield stress measurements produced low values (less than 20 Pa) in comparison to typical shear stresses developed within the injector (order of magnitude of 10^{4} Pa), the power-law model describes well the fluid behavior and it can be used in the flow analysis due to its simplicity.

When the gel fluid passes through any kind of injector it is subjected to significant shear stress and shear rate, and the mean apparent shear viscosity at the injector exit plane decreases. The mean apparent viscosity at the injector exit plane is given by [13]:

$$\overline{\eta} = 2K \cdot \int_{0}^{1} \left(\frac{r}{R}\right) \cdot \dot{\gamma}^{n-1} \cdot d\left(\frac{r}{R}\right) \tag{4}$$

Knowledge of the velocity and the velocity gradient of the injector flowfield can provide the strain rate, $\dot{\gamma}$, values and consequently the mean apparent viscosity at the injector exit plane. Either an analytical [13] or a numerical [14] solution can be utilized for this purpose. The model assumes steady, two-dimensional, axisymmetric, incompressible, laminar and isothermal flow of a power-law fluid in a convergent tube with no-slip conditions at the wall.

There is no doubt that the mean apparent shear viscosity plays an important role in gel atomization [8] at least in viscoinelastic gels. Therefore, the rheological properties, i.e. the mean apparent viscosity at the injector exit plane and the atomization characteristics can be correlated.

ATOMIZATION CHARACTERISTICS

The present study includes the spatial characterization of the spray resulting from a triplet-type atomizer and a parametric investigation to verify the effects of the following parameters on the droplet size (D_{32} – Sauter Mean Diameter) and flow number (FN):

- The gel mass flow rate;
- The gellant content;
- The atomizer geometry;
- The air to liquid ratio (ALR);
- The gel mean apparent viscosity at the injector exit plane;

Spatial Spray Characterization

In order to characterize the spray spatially, measurements were made at various axial (x) and radial (r) positions for several atomizer head orientations (ϕ).

The SMD change with the axial position downstream of the injector exit for different fluids is shown in Fig. 5. Up to 5 cm from the injector exit, for all fluids, SMD decreases as the spray moves downstream and droplet breakup occurs. For ungelled water, SMD almost does not change after 3 cm, indicating that no liquid evaporation takes place. As regards gels, in general, it must be kept in mind that heat of vaporization increases with increasing gelling agent content [16], which means that if evaporation does not occur in plain water, it certainly will not happen in gelled water, as in the present case. The reduction of SMD should be accounted to droplet breakup. However, for the gels, SMD increases after 5 cm and the

question that rises is if this is due to droplet coalescence or not. The answer is not straightforward. Examination of the raw data of the droplet number histograms shows that the number of large droplets is small although they carry a significant fraction of the liquid mass and this fraction decreases continuously as we move downstream. The Malvern Mastersizer is capable of detecting droplets up to 600 μm and there is a possibility that a few, larger than 600 μm, droplets may exist in positions further than 5 cm and they are not detected. If this is the case, then the increase of SMD after 5 cm may be attributed to the breakup of the previously undetected droplets rather than coalescence of gel droplets, although this option may also be feasible.

The SMD of water-gel (0.5% gellant) of $\dot{m}_{gel} = 1\,g/s,\ \dot{m}_{gas} = 5.3\,g/s,\ d = 0.42\,mm$ at various axial distances for different radial positions and injector head orientations is shown in Figs. 6 and 7 respectively and in Table 2. The volume droplet size distributions are presented in Figs. 8 (a-d) and 9 (a-c). It is quite clear that the spatial droplet size distribution is non-axisymmetric. Near the injector head most droplets are large. In Fig. 8a at x=2, the specific size distribution indicates that the droplet size exceeds the instrument maximum detection size therefore droplets larger than 600 μm are not detected. As we move downstream, the large droplets break up and/or move to the sides. Figure 7, which shows the SMD dependence on the injector head orientation, and Fig. 9 provide further evidence of the non-axisymmetric character of the spray and the tendency of the large droplets to move aside due to the radial momentum of the gas (also non-axisymmetric). The result is that at the centerline the droplets are smaller and they decrease in size by moving downstream.

The SMD of water-gel (0.5% gellant) of $\dot{m}_{gel} = 10.5\,g/s, \dot{m}_{gas} = 8.8\,g/s, d = 1.6\,mm$ for various gas impingement angles measured at the centerline is presented in Table 3 and Fig. 10. In general, increasing the jet impingement angle causes the droplet size to increase. This

is due to the fact that since the jet collision point is the same in all impingement angles, as β increases, the distance that the gas travels increases proportionally to 1/cosβ and the momentum loss results in ineffective liquid (gel) breakup. Therefore, it seems logical that low jet impingement angles are preferable.

The effect of gel mass flow rate on flow number and droplet size

Increasing the liquid mass flow rate at constant nitrogen flow causes SMD to increase as expected (Fig.11). Again, increasing the gellant content in the liquid increases the apparent viscosity of the liquid thus resulting in coarser atomization. Furthermore, examination of the Flow Number, FN, defined in Eq. (5) shows (Fig. 12) that for the same liquid mass flow rate, the required injection pressure in the atomizer increases ($FN \propto (\Delta p)^{-0.5}$, $\Delta p=p_{inj}-p_{amb}$, $p_{amb}=1$ atm) with increasing the gellant content.

$$FN = \frac{\dot{m}_l}{\sqrt{\Delta p}} \qquad (5)$$

The realization of the effect of the atomizer geometry on SMD is not an easy task. The examination of the effect of the gel passage convergence angle requires the use of atomizers that provide the same fluid mass flow rate at the same pressure drop while convergence angle varies. This means that for a constant (8 mm) length converging passage, the inlet and exit diameters differ in each atomizer and a trial and error process is necessary, while manufacturing a large number of atomizers is not feasible. In this case, the effect of the convergence angle is investigated by a different approach. The SMD of both 30^o and 2^o convergence angles seems to be quite similar for the same fuel mass flow rate (Fig. 13). However, the Flow Number in the 2^o angle case is significantly lower than the 30^o angle, i.e. the required injection pressure decreases by almost 40% (Fig. 14) when the wide angle is used. This result is consistent with the theoretical predictions of Rahimi and Natan [13-14].

The effect of air to liquid ratio

For a constant gas mass flow rate, increasing the gel mass flow rate produces larger droplets and this is shown in Fig. 15. In general, SMD exhibits a tendency to decrease with increasing ALR and this is in agreement with the measurements of Mansour and Chigier [8] for non-Newtonian liquids with a coaxial injector. This tendency is shown in both Fig. 16 (SMD vs. 1+1/ALR for different gas mass flow rates) and Fig. 17 (SMD vs. 1+1/ALR for different gellant contents). It must be kept in mind that the water gels used in the present research are shear-thinning, pseudoplastic fluids with low yield stress, and their behavior with increasing ALR is similar to this of Newtonian fluids. Still, it is more difficult to atomize gelled water than ungelled water. As the gellant content increases, its viscosity increases, consequently the breakup tendency decreases and this results in larger SMD values. In general, non-Newtonian fluids are more difficult to atomize in comparison to Newtonian fluids and perhaps, the plastic and elastic branches of a non-Newtonian gel fluid might pose a barrier to fine atomization.

Taking into account the gellant content and the injector geometry, SMD is correlated to ALR by the relation:

$$SMD = C \cdot \left(1 + 1/ALR\right)^4 \qquad (6)$$

Factor C includes the effect of the gellant content and the injector geometry and it was determined for each test-series. The correlation in Eq. (6) is shown in Fig. 18.

The effect of the gel mean apparent viscosity

In general, increasing the gel mass flow rate results in increasing SMD. However, this effect is not straightforward. For a constant geometry injector, increasing the mass flow rate produces higher stresses and strain rates, therefore reducing the mean apparent viscosity of the gel at the injector exit plane [13-14]. This is shown in Fig. 19 for 0.5% water-gel, d=0.42

mm. Consequently, SMD is governed by these two counteracting effects; the gel resistance to breakup increases due to the increased mass flow rate and decreases due to the lower viscosity value. In an effort to separate these effects, the mean apparent viscosity value at the injector exit plane was calculated employing the code of Ref. [14] for the corresponding experimental data and SMD was correlated, using a linear regression, to gas and gel mass flow rates and viscosity. This correlation is presented in Fig. 20 and it is described by:

$$SMD = A \cdot \dot{m}_{gas}^{-0.8} \cdot \dot{m}_{gel}^{2.34} \cdot \overline{\eta}_{gel}^{0.92} \qquad (7)$$

Correlations (6) and (7) were established for pure water and gels with gellant content of 0.5% and 1% for $\dot{m}_{gel} = 1.7 - 17.5\ g/s$, $\dot{m}_{gas} = 2.3 - 14.7\ g/s$, $d = 0.42 - 1.6\ mm$.

The importance of this result is significant because the rheological parameters, which cannot be measured at the injection point, can be now considered for the SMD estimation.

CONCLUSIONS AND FINAL REMARKS

In the present research, an effort was made to relate the rheological properties of gel fuel simulants with their atomization behavior. The gels were atomized using a triplet impinging air-blast atomizer. Droplet size distribution was measured using a Malvern Mastersizer X.

- Water-gels, which are considered as shear-thinning pseudoplastic fluids with low yield stress, exhibit similar spray patterns to Newtonian liquids, however, they are more difficult to atomize.
- Spatial distributions indicate that the spray pattern is non-axisymmetric.
- The Sauter Mean Diameter (SMD) decreases along the injector axis and increases with increasing the radial coordinate and the angle between the gas jets plane and the horizontal plane.

- Wide-angle convergent injectors require lower injection pressures to achieve the same atomization performance with regular triplet atomizers. The measurements imply that minimum drop-size distributions can be achieved by using certain impingement angles of the gas jets.
- Small impingement angles of the gas jets were found to provide better atomization.
- Atomization is significantly affected by the gellant content in the fuel and the injector geometry. The SMD of the spray increases with increasing the gellant content due to the respective increase of the shear viscosity.
- SMD was found to decrease with increasing air to liquid ratio and a correlation between SMD and ALR was found.
- The effect of the mean apparent viscosity at the injector exit plane on the spray droplet size was investigated employing a numerical code.
- SMD was found to decrease with decreasing the gel viscosity at the injector exit.
- Increasing the gel mass flow rate resulted in decreasing viscosity, however, the overall spray SMD was found to increase..
- A correlation between SMD gel and gas mass flow rates and gel viscosity was established.

REFERENCES

1. B. Natan and S. Rahimi, The Status of Gel Propellants in Year 2000, in K. K. Kuo and L. deLuca (ed.), *Combustion of Energetic Materials*, pp. 172-194, Begell House, Boca Raton, 2002.
2. J.D. Guglielmi, Atomization of JP-10 /B4C Gelled Slurry Fuel, M.Sc. Thesis, Naval Postgraduate School, Monterey, CA, 1992.

3. B.C. Urbon, Atomization and combustion of a Gelled, Metallized Slurry Fuel, M.Sc. Thesis, Naval Postgraduate School, Monterey, CA, 1992.
4. M.J. Green, D.C. Rapp and J. Roncace, Flow Visualization of a Rocket Injector Spray Using Gelled Propellant Simulants, AIAA paper 91-2198, June 1991.
5. K.T. Chojnacki and D.A. Feikema, Atomization Studies of Gelled Liquids, AIAA paper 94-2773, June 1994.
6. K.T. Chojnacki and D.A. Feikema, Atomization Studies of Gelled Bipropellant Simulants Using Planar Laser Induced Fluorescence, AIAA paper 95-2423, July 1995.
7. K.T. Chojnacki and D.A. Feikema, Study of Non-Newtonian Liquid Sheets Formed by Impinging Jets, AIAA paper 97-3335, July 1997.
8. A. Mansour A. and N. Chigier, Air-blast atomization of non-Newtonian liquids, *J. Non-Newtonian Fluid Mechanics*, vol. 58, pp. 161-194, 1995.
9. R.W. Dexter, Measurement of extensional viscosity of polymer solutions and its effects on atomization from a spray nozzle, *Atomization and Sprays*, vol. 6, pp. 167-191, 1996.
10. M.E. Teske and J. Bilanin, Drop size scaling analysis of Non-Newtonian Fluids, *Atomization and Sprays*, vol. 4, pp. 473-483, 1994.
11. A.L. Yarin, E. Zussman, A. Theron, S. Rahimi, Z. Sobe, and D. Hasan, Elongational behavior of gelled propellant simulants, *J. Rheology*, vol. 48, No. 1, pp. 101-116, 2004.
12. A.L. Yarin, Free liquid jets and films: hydrodynamics and rheology, Longman Scientific & Technical with John Wiley & Sons, New-York, 1993.
13. S. Rahimi and B. Natan, The flow of Gel Fuels in Tapered injectors, *J. Propulsion and Power*, vol. 16, No. 3, pp. 458-471, 2000.
14. S. Rahimi and B. Natan, Numerical Solution of the Flow of Power-Law Gel Propellants in Converging Injectors, *Propellants Explosives and Pyrotechnics*, vol. 25, No. 4, pp. 203-212, 2000.

15. S. Rahimi and B. Natan, On the Thixotropic Effect of Inorganic Gel Fuels," *J. Propulsion and Power*, vol. 16, No. 6, pp. 1182-1184, 2000.

16. G. Nachmoni and B. Natan, Combustion Characteristics of Gel Fuels, *Combustion Science and Technology*, vol. 156, pp. 139-157, 2000.

NOMENCLATURE

A	correlation factor
ALR	Air to Liquid mass Ratio
C	correlation factor
d	exit diameter
D	droplet diameter
De	Deborah Number
F	fuel
FN	Flow Number
K	power-law consistency index
L	Distance between impingement point and the injector face
$\dot{m}$	mass flow rate
n	power-law rate index
Ni	droplet number
O	oxidizer
p	pressure
R	Radius
SMD (D_{32})	Sauter Mean Diameter
x, r, ϕ	cylindrical coordinates
X, Y, Z	Cartesian coordinates
α	convergence angle
β	impingement angle
$\dot{\gamma}$	shear rate
η	non-Newtonian viscosity
$\overline{\eta}$	mean apparent viscosity
τ	shear stress
τ_{HB}	Herschel-Bulkley yield stress

Subscripts

amb	ambient
gas	gas
inj	injection
l	liquid

FIGURE CAPTIONS

Fig. 1. Elaborated layout of the experimental facility of gel propellant atomization

Fig. 2. Spray pattern measurements

Fig. 3. The injector geometry

Fig. 4. Flow curves for gel propellant simulants with different gellant content

Fig. 5. Sauter Mean Diameter vs. axial position, $\dot{m}_l$ =4.6 g/s, d=0.42 mm, r=0, $\phi=0^o$, $\alpha=6^o$, $\beta=70^o$, L=8 mm

Fig. 6. Sauter Mean Diameter vs. axial position at various radial locations, 0.5% water-gel, $\dot{m}_{gel}$ =1 g/s, $\dot{m}_{gas}$ =5.3 g/s, d=0.42mm, $\phi=0^o$, $\alpha=6^o$, $\beta=70^o$, L=8 mm

Fig. 7. Sauter Mean Diameter vs. axial position at various head orientations, 0.5% water-gel, $\dot{m}_{gel}$ =1 g/s, $\dot{m}_{gas}$ =5.3 g/s, d=0.42mm, r=0, $\alpha=6^o$, $\beta=70^o$, L=8 mm

Fig. 8. Volume drop size distribution along the injector axis, 0.5% water-gel, $\dot{m}_{gel}$ =1 g/s, $\dot{m}_{gas}$ =5.3 g/s, d=0.42mm, $\phi=0^o$, $\alpha=6^o$, $\beta=70^o$, L=8 mm (a) center line, (b) r=1cm, (c) r=2cm, (d) r=3cm

Fig. 9. Volume drop size distribution along the centerline at various injector head orientations, 0.5% water-gel, $\dot{m}_{gel}$ =1 g/s, $\dot{m}_{gas}$ =5.3 g/s, d=0.42mm, r=0, $\alpha=6^o$, $\beta=70^o$, L=8 mm, (a) $\phi=30^o$, (b) $\phi=60^o$, (c) $\phi=90^o$

Fig. 10. Sauter Mean Diameter vs. gas impingement angle at the centerline for various axial positions, 0.5% water-gel, $\dot{m}_{gel}$ =10.5 g/s, $\dot{m}_{gas}$ =8.8 g/s, d=1.6mm, $\phi=0^o$, $\alpha=6^o$, L=12 mm

Fig. 11. Sauter Mean Diameter vs. gel mass flow rate,
$\dot{m}_g$=8.7 g/s, d=1.6 mm, x=6 cm, r=0, ϕ=0^o, α=30°, β=70^o, L=8 mm

Fig. 12. Flow number vs. gel mass flow rate,
$\dot{m}_g$=8.7 g/s, d=1.6 mm, x=6 cm, r=0, ϕ=0^o, α=30°, β=70^o, L=8 mm

Fig. 13 Sauter Mean Diameter vs. gel mass flow rate, 0.5% Water gel,
$\dot{m}_g$=8.7 g/s, d=1.6 mm, x=6 cm, r=0, ϕ=0^o, β=70^o, L=8 mm

Fig. 14. Flow Number vs. gel mass flow rate, 0.5% Water gel
$\dot{m}_g$=8.7 g/s, d=1.6 mm, x=6 cm, r=0, ϕ=0^o, β=70^o, L=8 mm

Fig. 15. Volume droplet size for various gel mass flow rates, 0.5% water-gel,
$\dot{m}_g$=9.2 g/s, d=0.42 mm, x=5 cm, r=0, ϕ=0^o, α=6°, β=70^o, L=8 mm

Fig. 16. Sauter Mean Diameter vs. (1+1/ALR) for various conditions, 0.5% water-gel,
d=0.42 mm, x=5 cm, r=0, ϕ=0^o, α=6°, β=70^o, L=8 mm

Fig. 17. Sauter Mean Diameter vs. (1+1/ALR) for various gels,
d=0.82 mm, $\dot{m}_{gas}$=7.2g/s, x=5 cm, r=0, ϕ=0^o, α=30°, β=70^o, L=8 mm

Fig. 18. Correlation of the Sauter Mean Diameter with Air-to-Liquid Ratio, x=5 cm

Fig. 19. Mean apparent viscosity at the injector exit vs. gel mass flow rate,
0.5% water-gel, d=0.42 mm, α=6°

Fig. 20. Correlation of the Sauter Mean Diameter with the mean apparent viscosity at the exit and with the gel and gas mass flow rates

Table 1 Rheological parameters of gel propellant simulants

Gellant (%)	Power Law Model		Herschel Bulkley Model		
	n	K, Pa-s^n	n	K, Pa-s^n	τ_{HB}, Pa
0.3	0.41	10.1	0.44	7.9	4.4
0.5	0.39	18.2	0.42	13.9	7.4
0.75	0.40	21.7	0.44	16.8	9.7
1	0.39	29.2	0.42	22.6	12.8

Table 2 SMD (μm) distribution for various axial position of the injector for various radial and circumference orientations, $\dot{m}_{gas}$ =5.3 g/s, $\dot{m}_{gel}$ =1 g/s, d=0.42 mm, L=8 mm

Axial position, cm	r=0 cm, ϕ=0º	r=1 cm, ϕ=0º	r=2 cm, ϕ=0º	r=3 cm, ϕ=0º	r=0 cm, ϕ=30º	r=0 cm, ϕ=60º	r=0 cm, ϕ=90º
2	60.33	53.77	60.12	*No spray*	61.04	64.04	73.07
3	37.33	37.99	48.04	54.34	45.25	57.54	73.22
4	29.68	32.44	39.47	43.92	35.74	47.53	51.53
5	26.22	29.96	37.97	47.23	33.89	45.82	59.33
6	26.19	28.33	33.17	39.69	31.36	36.78	60.11

Table 3 SMD (μm) distribution for various gas impingement angles for various special orientations of the injector, d=1.6 mm, $\dot{m}_{gas}$ =8.8 g/s, $\dot{m}_{gel}$ =10.5 g/s, L=12 mm

Axial position, cm	Impingement angle and spatial orientation					
	β=50º, r=0 cm, ϕ=0º	β=60º, r=0 cm, ϕ=0º	β=70º, r=0 cm, ϕ=0º	β=80º, r=0 cm, ϕ=0º	β=70º, r=1 cm, ϕ=0º	β=70º, r=0 cm, ϕ=30º
2	119.8	107	78.41	197.88	200.8	94.58
3	69.89	45	54.66	88.3	58.19	-
4	37.73	32.47	37.09	40.38	36.07	40.82
5	24.36	26.5	34.05	39.3	30.58	-
6	21.49	23.59	31.44	34.99	27.8	43.36

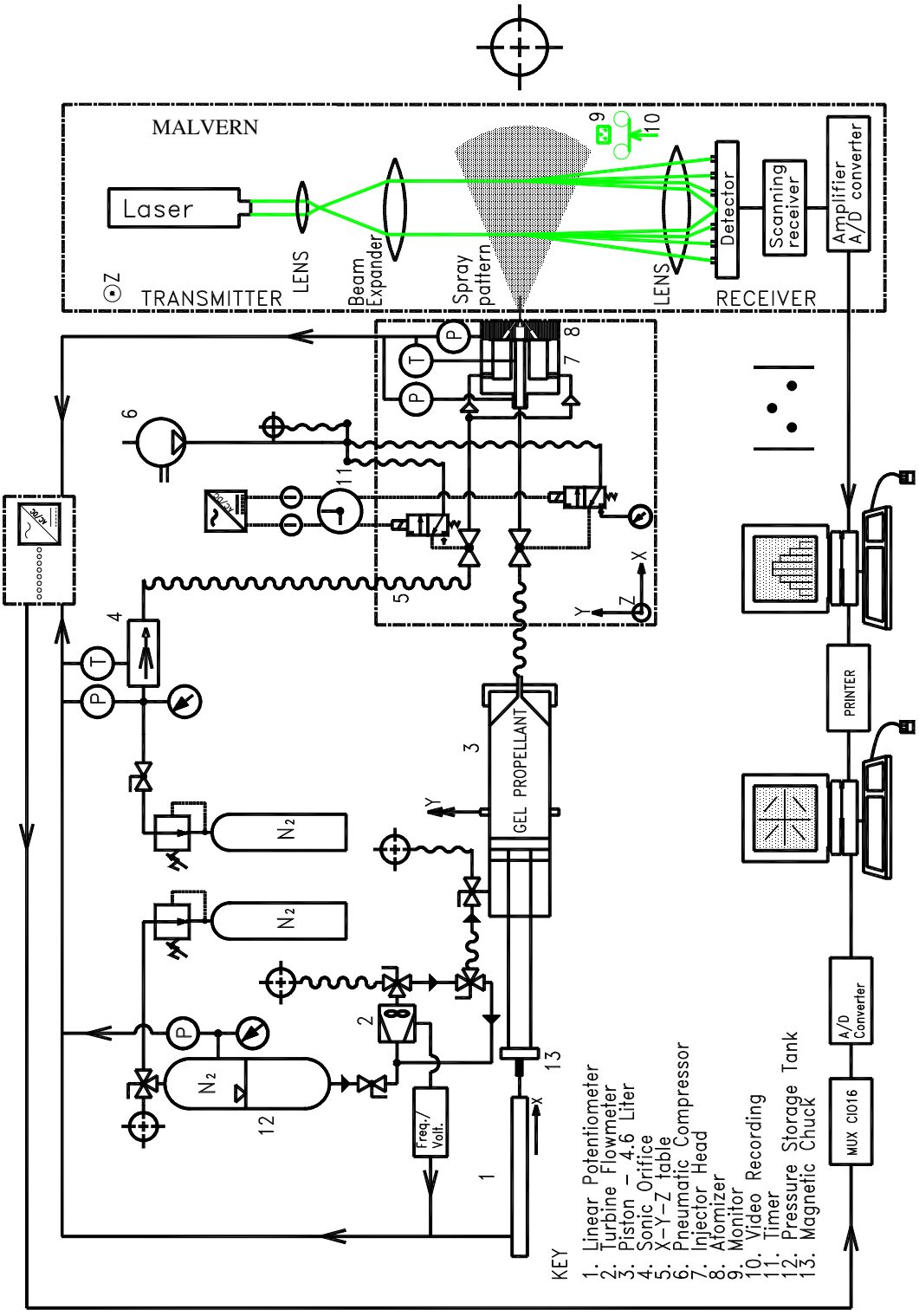

Fig. 1. Elaborated layout of the experimental facility of gel propellant atomization.

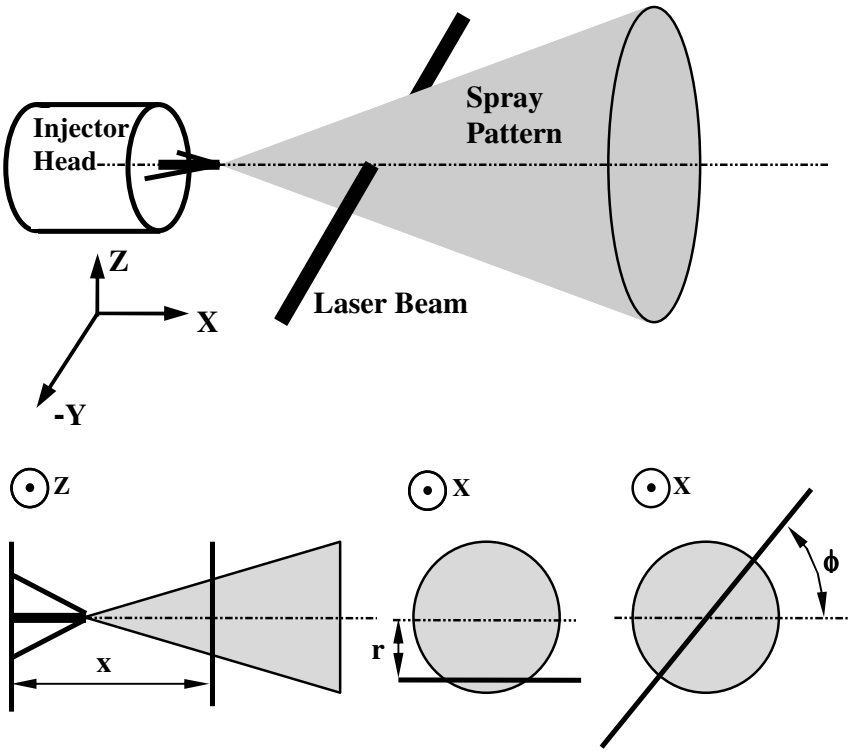

Fig. 2. Spray pattern measurements.

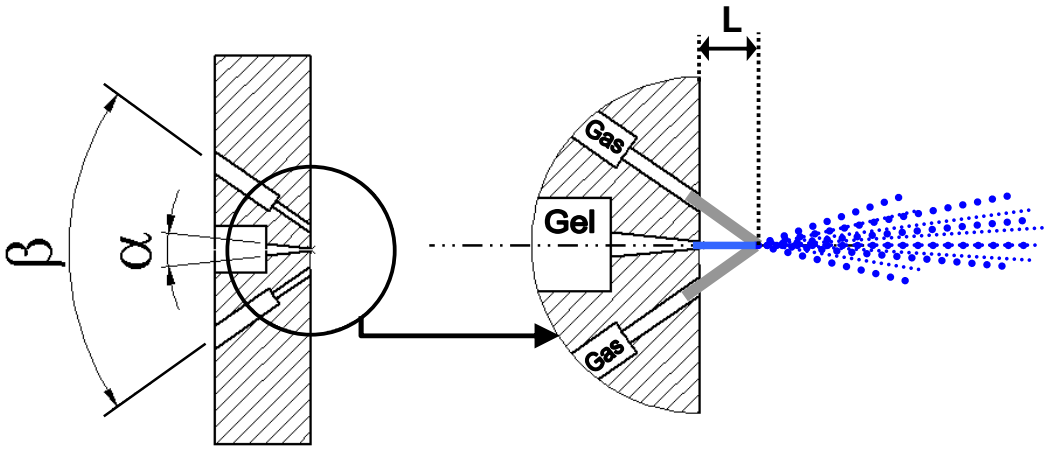

Fig. 3. The injector geometry.

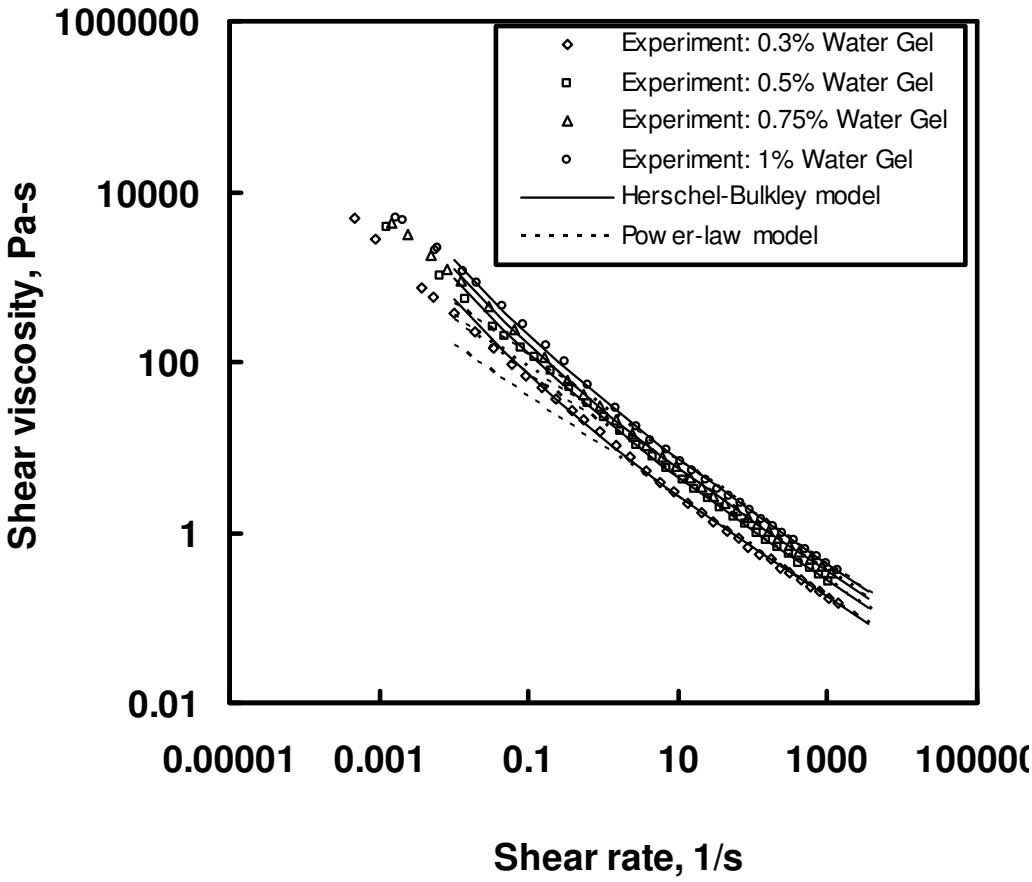

Fig 4. Flow curves for gel propellant simulants with different gellant content.

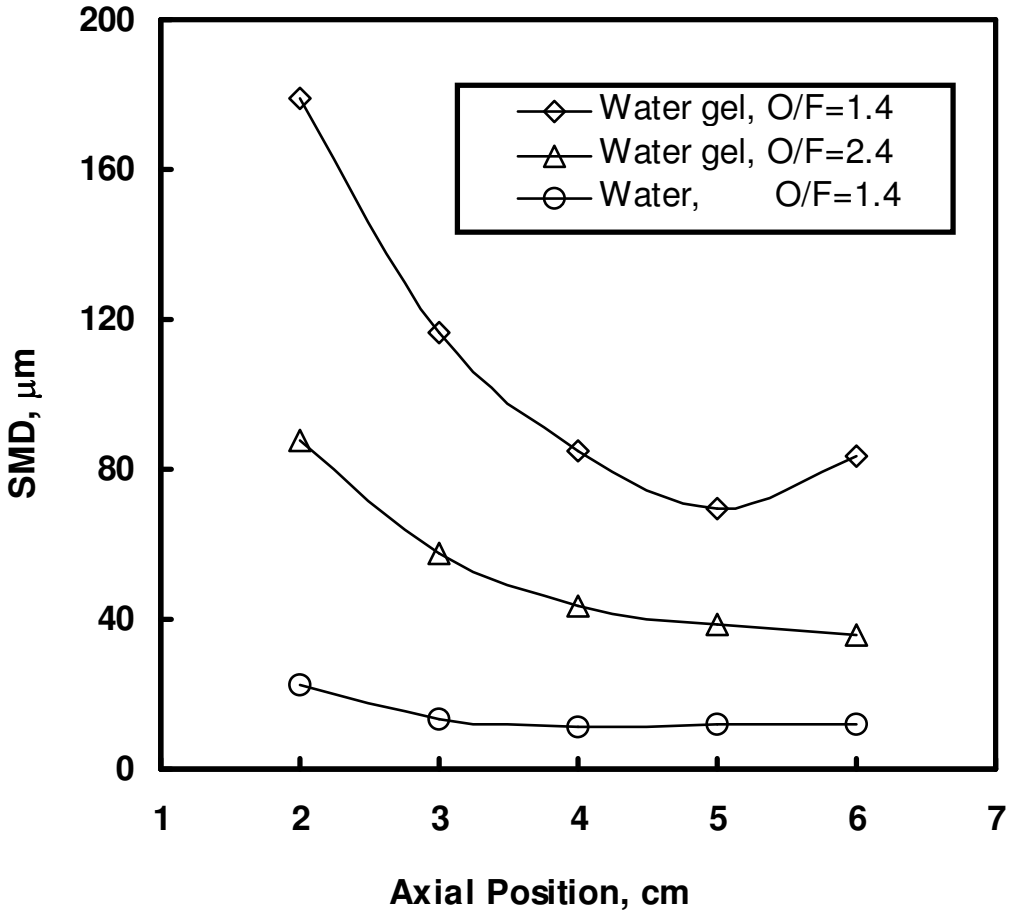

Fig. 5. Sauter Mean Diameter vs. axial position, $\dot{m}_l$ =4.6 g/s, d=0.42 mm, r=0, $\phi=0^o$, $\alpha=6^o$, $\beta=70^o$, L=8 mm

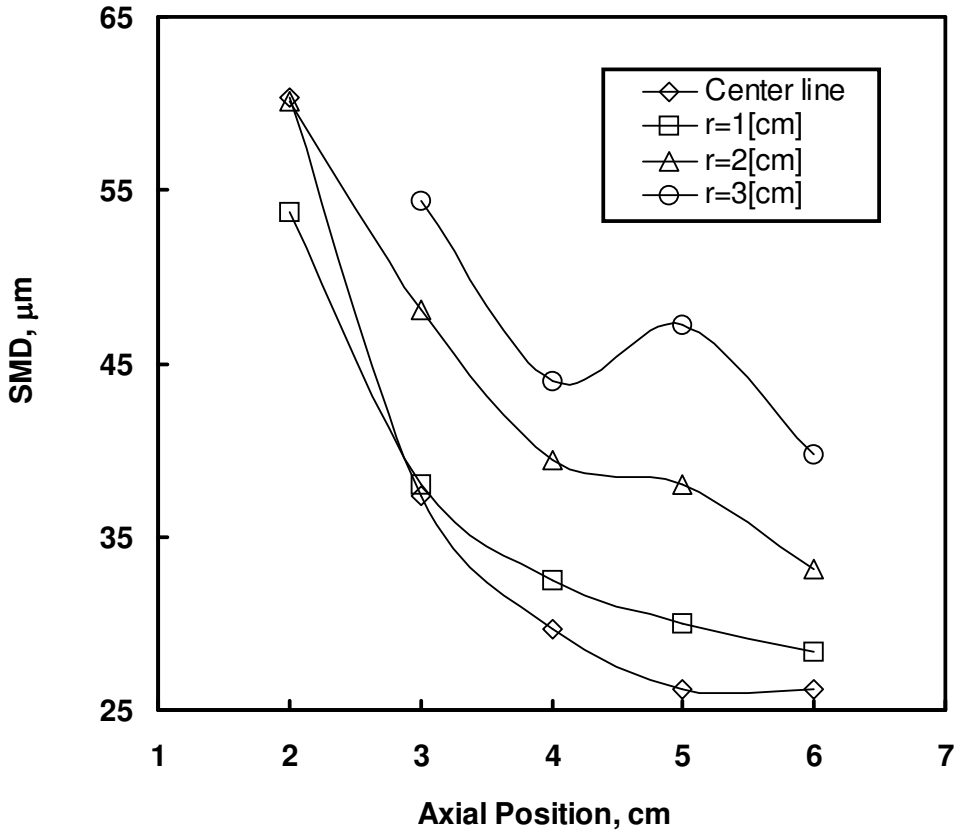

Fig. 6. Sauter Mean Diameter vs. axial position at various radial locations,
0.5% water-gel, $\dot{m}_{gel}$ =1 g/s, $\dot{m}_{gas}$ =5.3 g/s, d=0.42mm
$\phi=0^o$, $\alpha=6^o$, $\beta=70^o$, L=8 mm

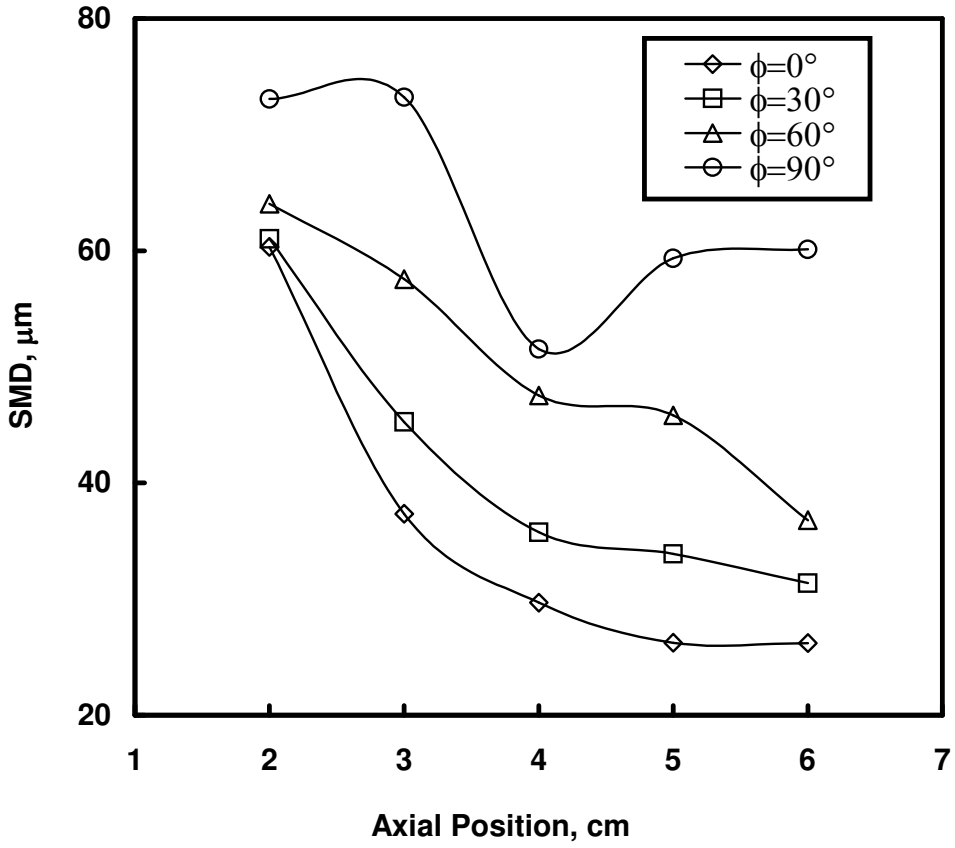

Fig. 7. Sauter Mean Diameter vs. axial position at various head orientations, 0.5% water-gel, $\dot{m}_{gel}$ =1 g/s, $\dot{m}_{gas}$ =5.3 g/s, d=0.42mm, r=0, $\alpha=6^{o}$, $\beta=70^{o}$, L=8 mm

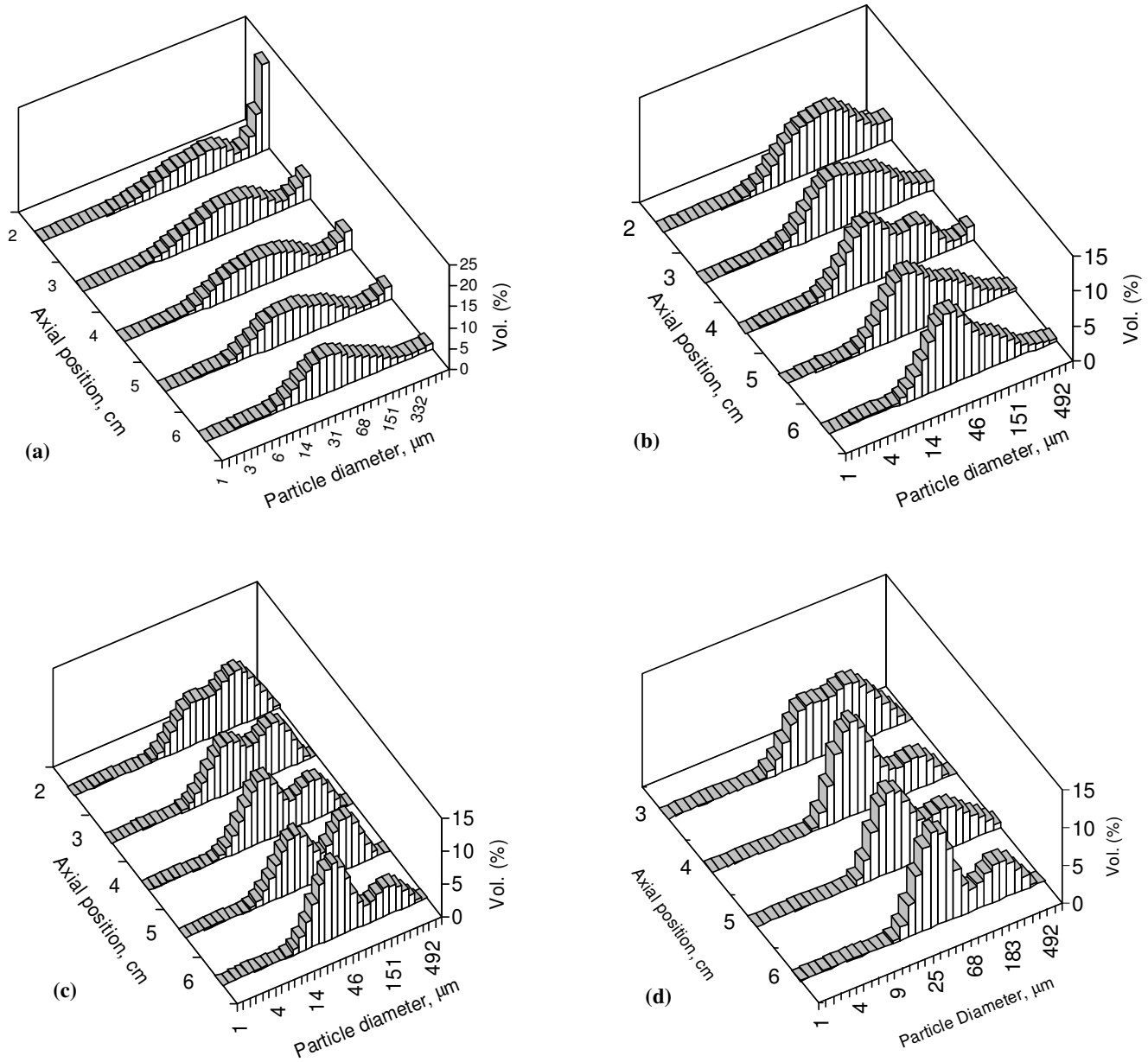

Fig. 8. Volume drop size distribution along the injector axis, 0.5% water-gel,
$\dot{m}_{gel}$ =1 g/s, $\dot{m}_{gas}$ =5.3 g/s, d=0.42 mm, $\phi=0^o$, $\alpha=6^o$, $\beta=70^o$, L=8 mm
(a) center line, (b) r=1cm, (c) r=2cm, (d) r=3cm.

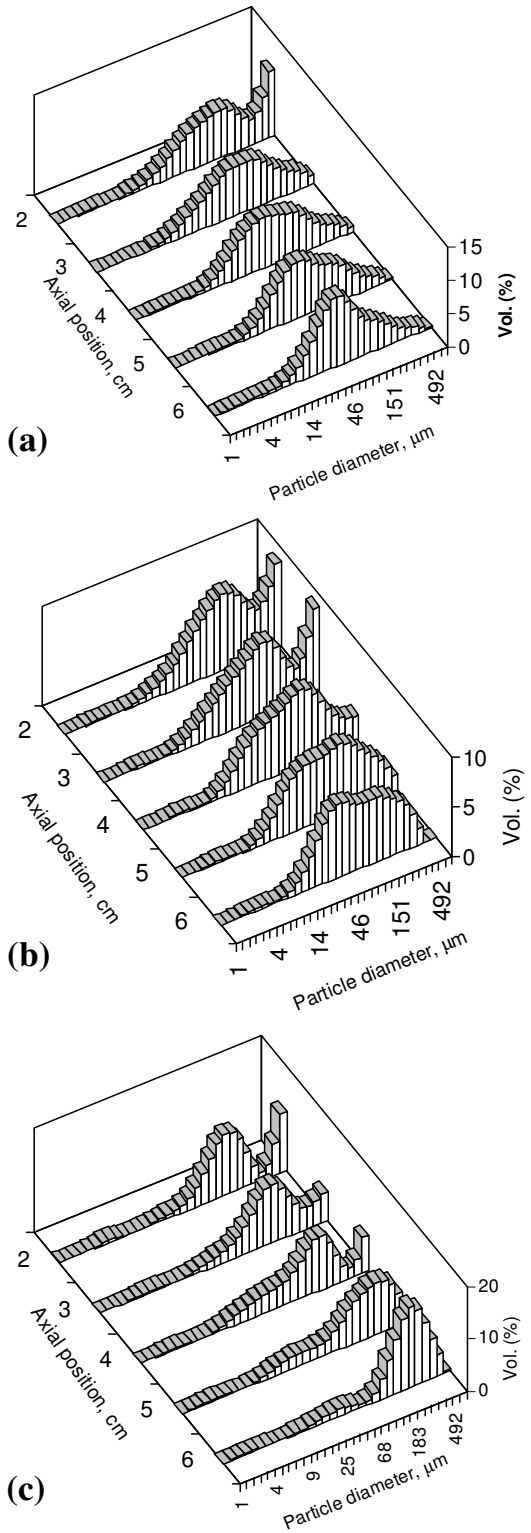

Fig. 9. Volume drop size distribution along the centerline at various injector head orientations, 0.5% water-gel, $\dot{m}_{gel}$=1 g/s, $\dot{m}_{gas}$=5.3 g/s, d=0.42 mm, r=0, $\alpha=6^{o}$, $\beta=70^{o}$, L=8 mm, (a) $\phi=30^{o}$, (b) $\phi=60^{o}$, (c) $\phi=90^{o}$

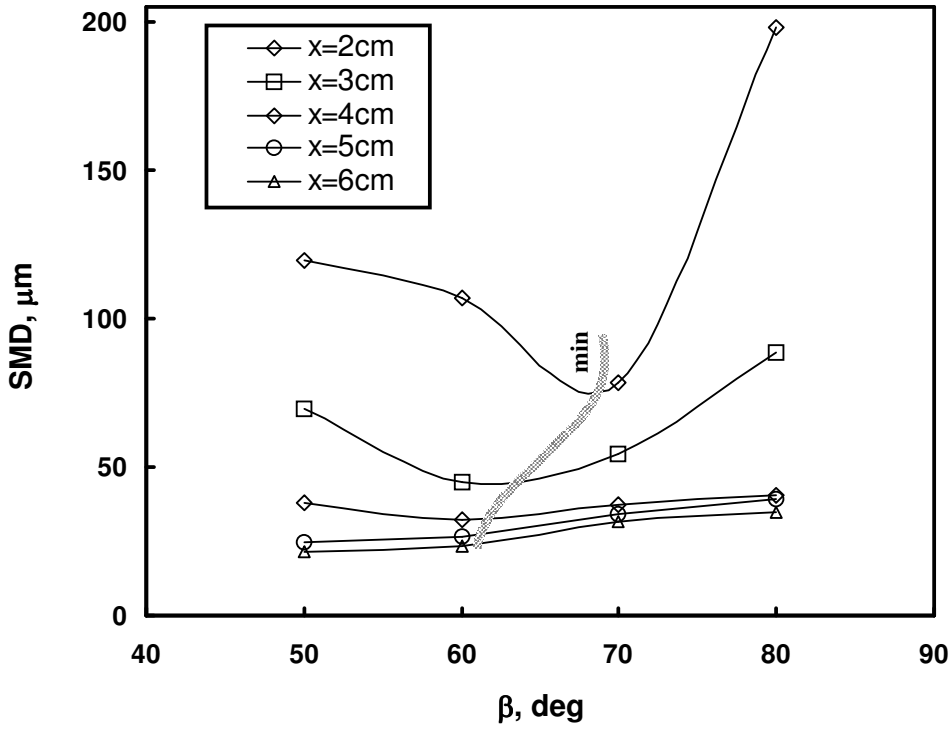

Fig. 10. Sauter Mean Diameter vs. gas impingement angle at the centerline for various axial positions, 0.5% water-gel, $\dot{m}_{gel}$ =10.5 g/s, $\dot{m}_{gas}$ =8.8 g/s, d=1.6 mm, ϕ=0°, α=6°, L=12 mm

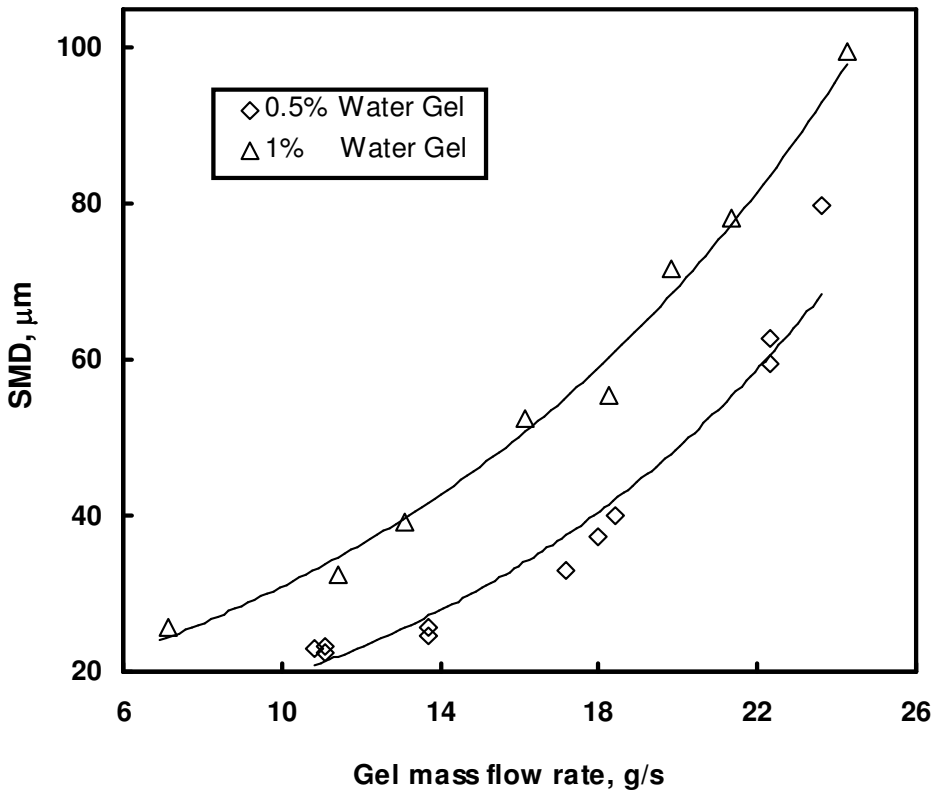

Fig. 11. Sauter Mean Diameter vs. gel mass flow rate,
$\dot{m}_g$ =8.7 g/s, d=1.6 mm, x=6 cm, r=0, ϕ=0^o, α=30°, β=70^o, L=8 mm

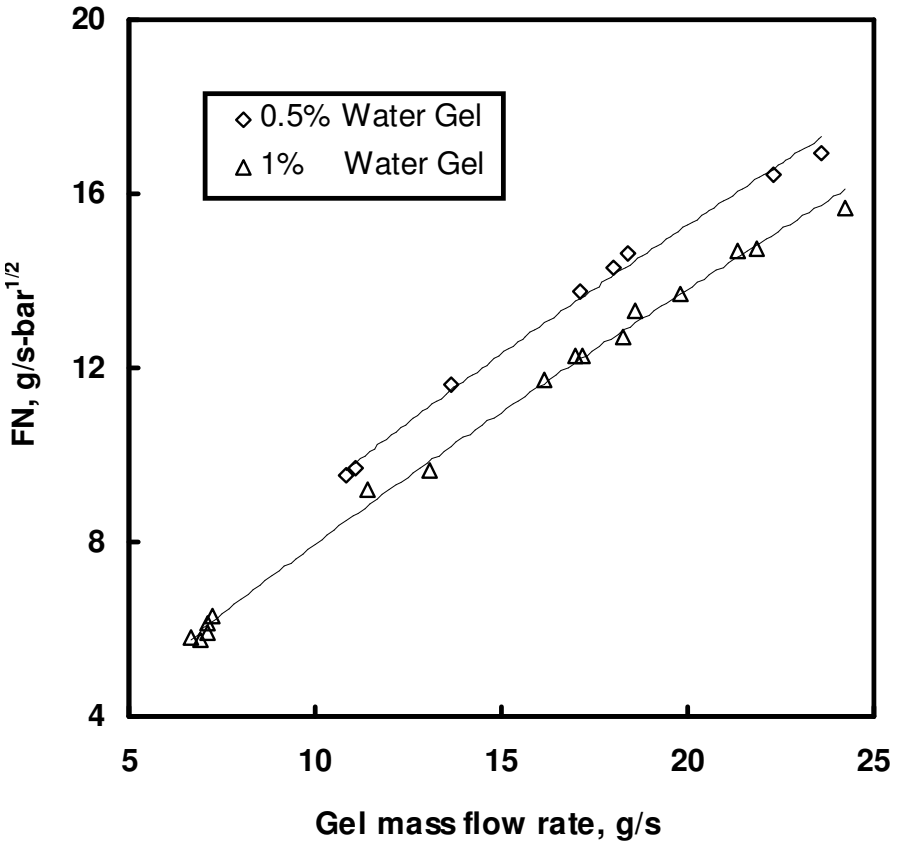

Fig. 12. Flow number vs. gel mass flow rate,
$\dot{m}_g$ =8.7 g/s, d=1.6 mm, x=6 cm, r=0, ϕ=0^o, α=30°, β=70^o, L=8 mm

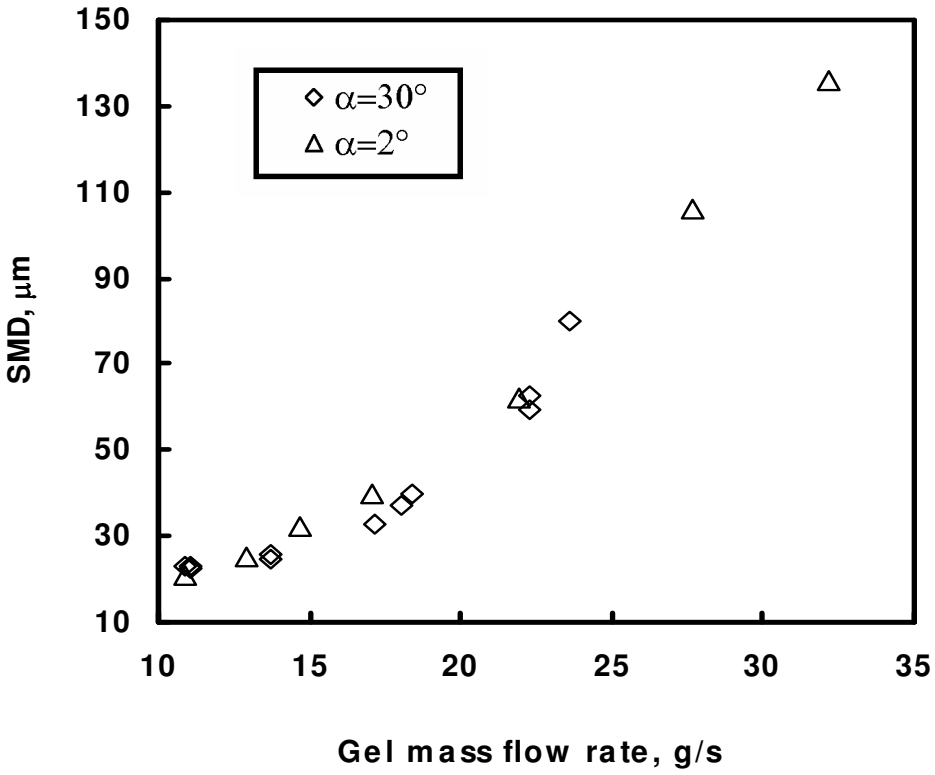

Fig. 13. Sauter Mean Diameter vs. gel mass flow rate, 0.5% Water gel, $\dot{m}_g$=8.7 g/s, d=1.6 mm, x=6 cm, r=0, ϕ=0^o, β=70^o, L=8 mm

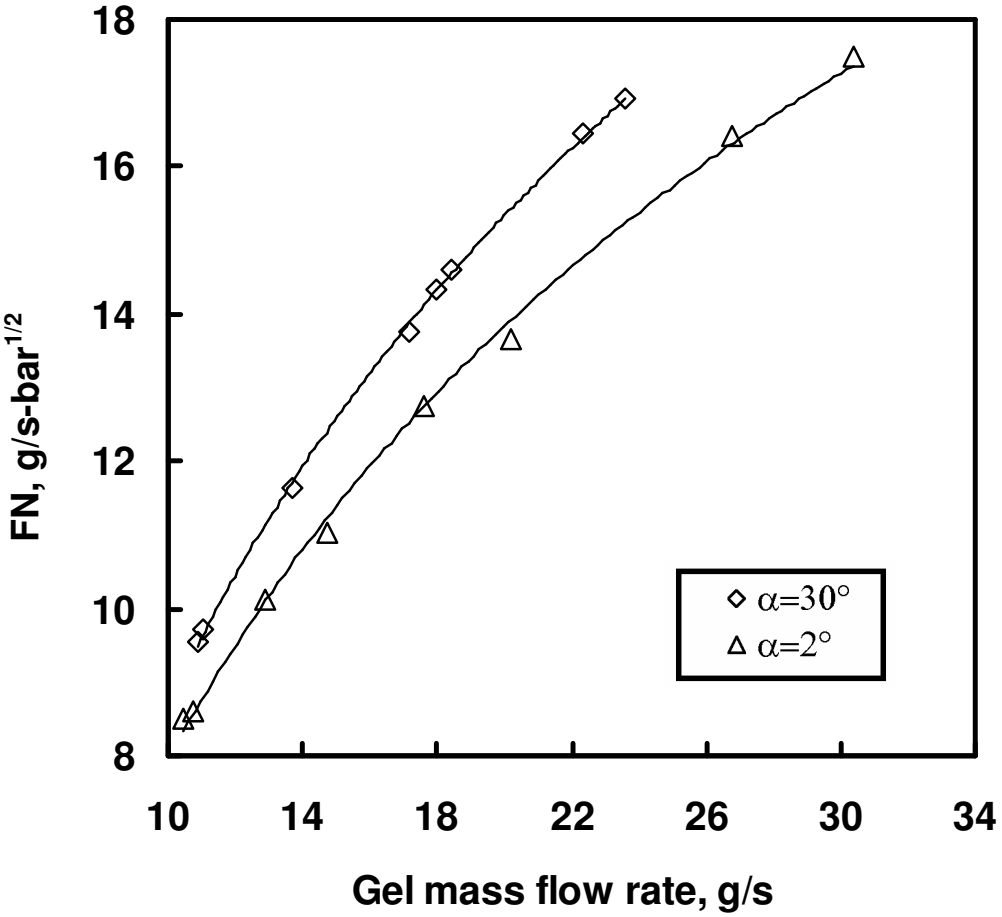

Fig. 14. Flow Number vs. gel mass flow rate, 0.5% Water gel
$\dot{m}_g$ =8.7 g/s, d=1.6 mm, x=6 cm, r=0, ϕ=0^o, β=70^o, L=8 mm

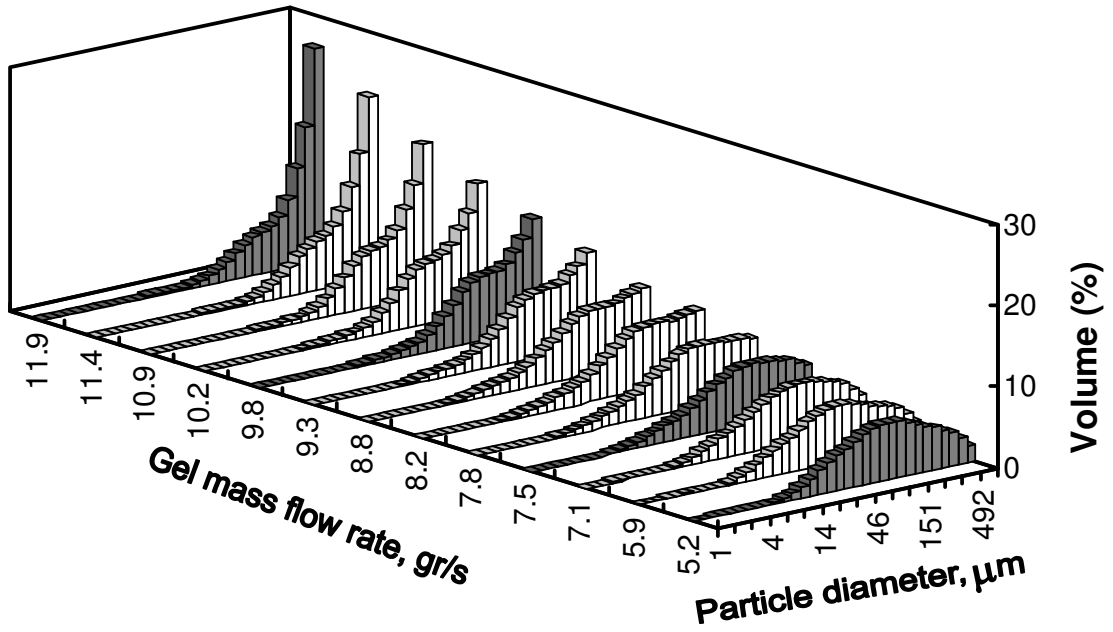

Fig. 15. Volume droplet size for various gel mass flow rates, 0.5% water-gel, $\dot{m}_g$ =9.2 g/s, d=0.42 mm, x=5 cm, r=0, ϕ=0^o, α=6°, β=70^o, L=8 mm

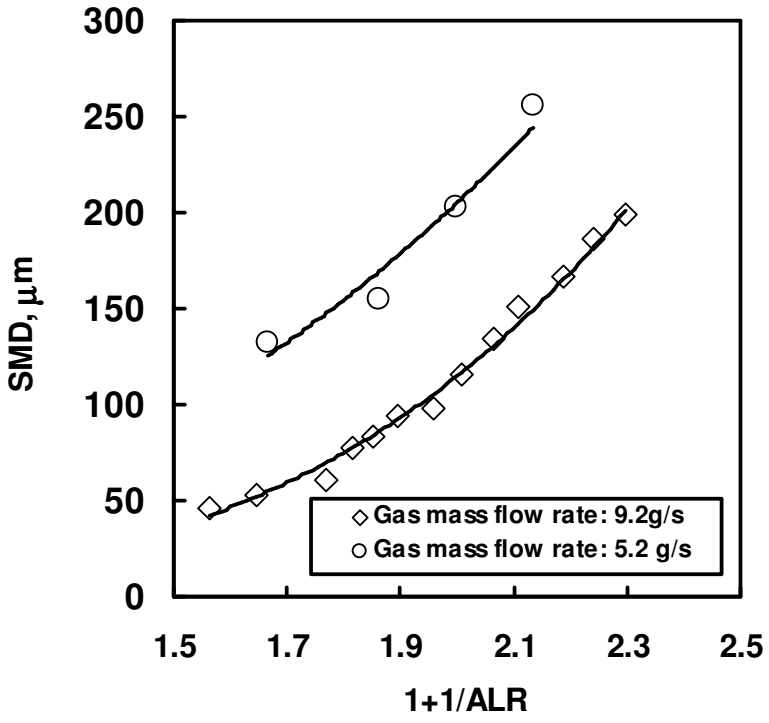

Fig. 16. Sauter Mean Diameter vs. (1+1/ALR) for various conditions, 0.5% water-gel, d=0.42 mm, x=5 cm, r=0, $\phi=0^{o}$, $\alpha=6°$, $\beta=70^{o}$, L=8 mm

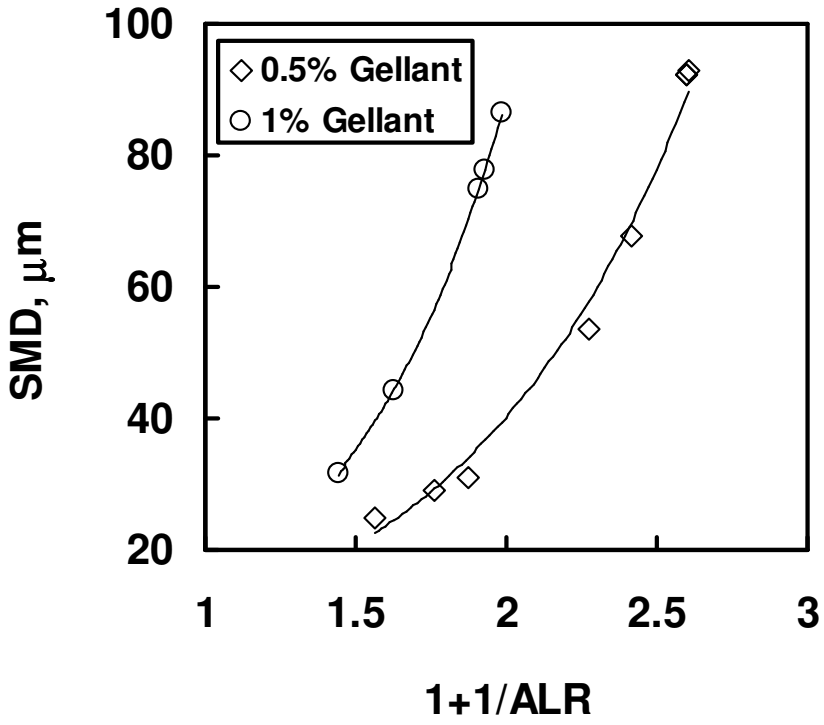

Fig. 17. Sauter Mean Diameter vs. (1+1/ALR) for various gels,
d=0.82 mm, $\dot{m}_{gas}$ =7.2g/s, x=5 cm, r=0, $\phi=0^{o}$, $\alpha=30°$, $\beta=70^{o}$, L=8 mm

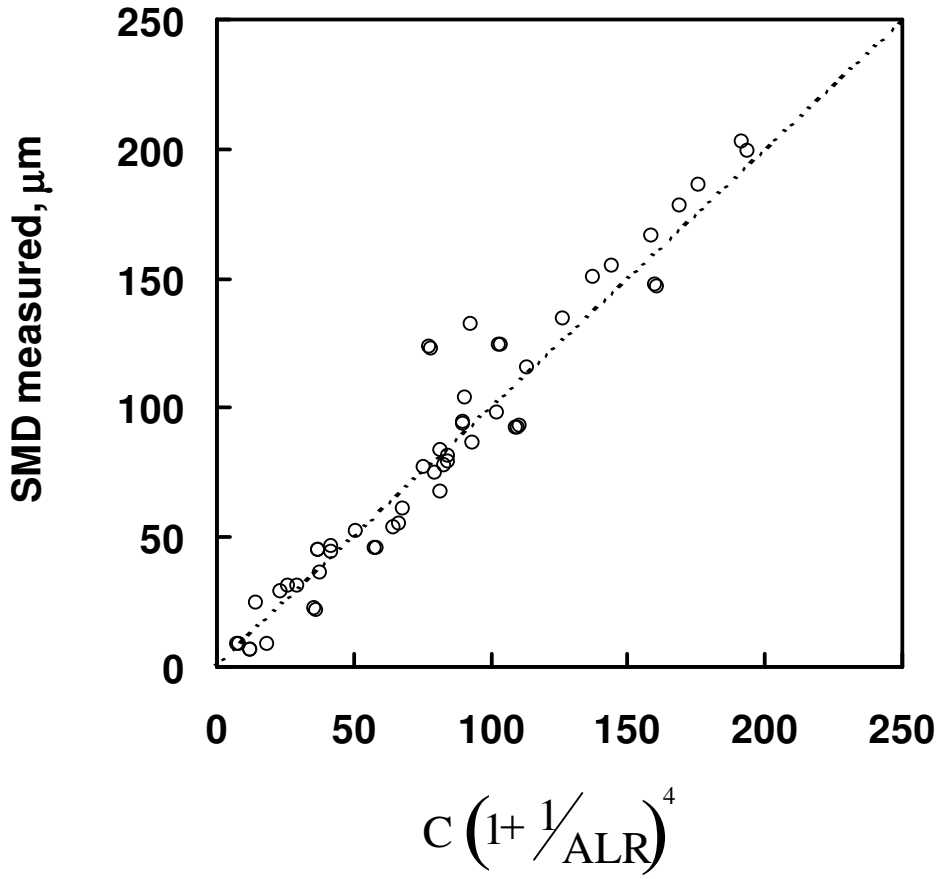

Fig. 18. Correlation of the Sauter Mean Diameter with Air-to-Liquid Ratio, x=5 cm.

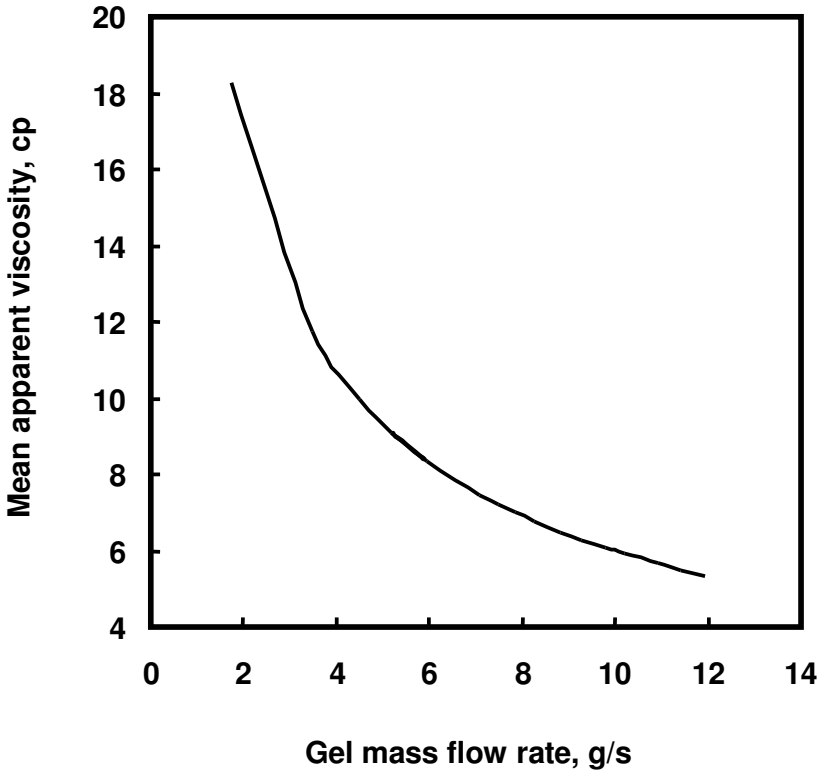

Fig. 19. Mean apparent viscosity at the injector exit vs. gel mass flow rate, 0.5% water-gel, d=0.42 mm, α=6°

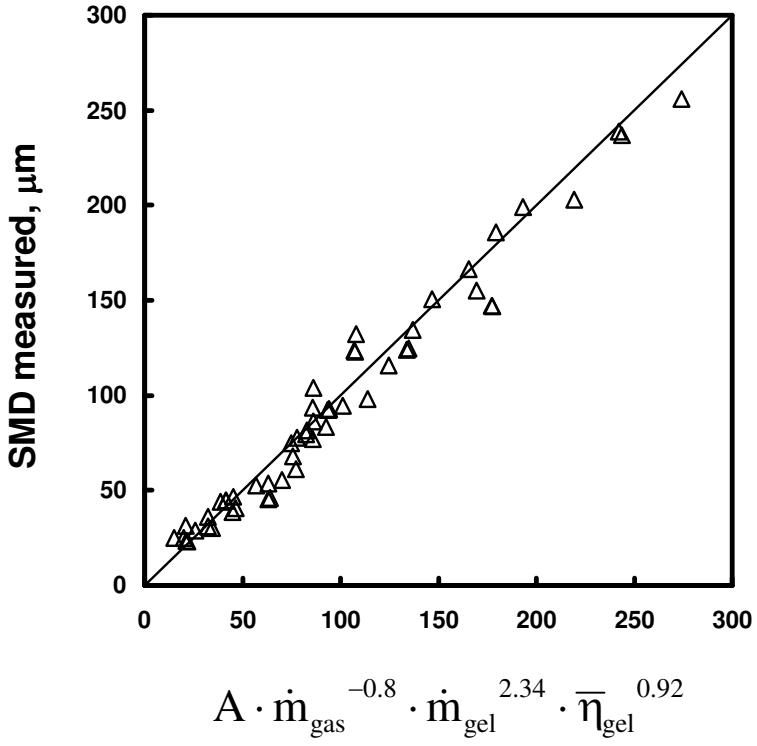

Fig. 20. Correlation of the Sauter Mean Diameter with the mean apparent viscosity at the exit and with the gel and gas mass flow rates.